Interaction model for design of geogrid pullout

F. Jacobs
RWTH Aachen University, Germany (jacobs@geotechnik.rwth-aachen.de)

ABSTRACT: The anchorage of geogrids in soil is designed, on the one hand, under the simplifying but arguable assumption of a constant interaction coefficient along the entire geogrid anchorage length. On the other hand, considerable and presumably positive effects caused by the deviations in a typical geogrid alignment are neglected. The existence of a multitude of safe structures designed this way might show that these two simplifications neutralize each other. However, as the pullout failure mode is actually decisive in anchorage trenches with low overburden, geogrid anchorage with trenches should be examined in more detail. In addition, with increasing requested service life durations up to 100 years, e.g., from German legislation, the required accuracy of the predicted material loading for all geogrid components increases as well.

Therefore, a model for the interaction between geogrid and soil has been developed at RWTH Aachen University with more than 120 pullout tests, which explicitly takes into account both load transfer mechanisms (i.e., friction and mobilized earth pressure in front of transverse tensile members). Additionally, an approach to include deviation effects within anchorage trenches has been formulated, which has been incorporated into the interaction model. In this paper, the model development is presented as well as its successful validation, first, with results from large pullout tests for the interaction model and, second, with field measurements from within a geogrid anchorage trench for the deviation effect approach.

Keywords: geogrid pullout, anchorage trench, interaction model, deviation forces

1 INTRODUCTION

Anchorage of geogrids in soil, as it occurs e.g. in reinforced retaining structures or surface-parallel systems, is described in many standards or recommendations regarding the ultimate limit state (e.g. German EBGEO, Deutsche Gesellschaft für Geotechnik, 2011; British Standard 8006, 2010; FHWA-NHI-00-043, US Department of Transportation, 2001), but serviceability limit states are not defined. Additionally, on the one hand, all of the guidelines assume a constant interaction coefficient along the anchorage length of a geogrid. At the same time, it is known that, due to the flexibility of the tensile geogrid products and the displacement-dependent load transfer mechanisms (i.e. friction and mobilized earth pressure in front of transverse tensile members), the mobilization of interaction varies along the geogrid anchorage length. In fact, the shear stresses in the front anchorage part can be disproportionately high, which has to be compatible with all geogrid components (see e.g. Palmeira, 2009; Ezzein & Bathurst, 2014). On the other hand, considerable, presumably positive effects caused by the deviations in a typical alignment of a geogrid in an anchorage trench are neglected (Briançon et al. 2000). The existence of a multitude of safe structures designed with these two simplifications might show that they neutralize each other. But as the failure mode *geogrid pullout* is actually decisive for the design of geogrid anchorages with low overburden, e.g., as part of liner systems of waste disposals, geogrid anchorage within trenches should be examined in more detail, including explicit consideration of both load transfer mechanisms (Müller, 2014). In addition, with increasing requested service life durations up to 100 years (e.g., German Landfill Ordinance, Bundesanzeiger Verlag 2009), the required accuracy of the predicted material loading for all geogrid components increases as well.

Therefore, an interaction model has been developed at RWTH Aachen University, which takes into account these two load transfer mechanisms. With a total of more than 120 pullout tests, the following influential parameters were investigated: soil type (sand and gravel), soil density, geogrid tensile strength and stiffness, geogrid aperture size and overburden pressure.

In this paper, first, the interaction model with an exemplary calibration result and its validation using results from pullout tests in a large box is presented. Second, an approach for the consideration of deviation effects in anchorage trenches is developed and then validated with field measurements from a geogrid anchorage trench of a liner system of a waste disposal.

2 INTERACTION MODEL GEOGRID/SOIL

The interaction model described below has been developed with more than 120 pullout tests, varying the following influential parameters: soil type (sand and two types of gravel), soil density, geogrid tensile strength and stiffness, geogrid aperture size and overburden pressure. Due to the limited space in this paper, only exemplary results can be shown and therefore it is forgone to give the entire test program and all exact material properties. The full study will be published elsewhere soon.

2.1 *Model development*

Within the model, the planar geogrid is modeled as one-dimensional and discretized into a finite number of elements along its main tensile direction as it is shown in Figure 1a (bottom). These elements are either pure frictional elements or frictional elements including a junction to a transverse tensile member where the bearing resistance in front of such a transverse tensile member is transferred to the longitudinal tensile member. Horizontal equilibrium at a longitudinal element with connected transverse tensile member as in Figure 1a (bottom) leads to the tensile force T_i at element i:

$$T_i = T_{i-1} + 2 \cdot L_e \cdot W_l \cdot \sigma_n \cdot \tan\left(\delta\left(u_{i-1}, \sigma_n\right)\right) \cdot n_g + T_{xmd,i}\left(u_{i-1}, \sigma_n\right) \quad (1)$$

where L_e = element length, W_l = width of longitudinal tensile member, σ_n = normal pressure on geogrid, $\delta(u_{i-1},\sigma_n)$ = mobilized contact friction angle between longitudinal tensile member and soil, u_{i-1} = displacement of element i-1, n_g = number of longitudinal geogrid tensile members per unit width, and $T_{xmd}(u_{i-1},\sigma_n)$ = mobilized bearing resistance in front of transverse tensile member.

The displacement of element i is calculated by:

$$u_i = u_{i-1} + \varepsilon\left(T_i\right) \cdot L_e \quad (2)$$

where $\varepsilon(T_i)$ = strain of longitudinal geogrid tensile member.

Decisive for a geogrid-soil interaction model is its description of the bearing resistance of transverse tensile members. Here, the model from Ziegler & Timmers (2004), as also proposed by Müller (2014), was chosen. As shown in Figure 1c, it assumes the displacement-dependent development of an earth pressure zone in front of each transverse tensile member with the length mob L. The bearing resistance T_{xmd} follows from the integrated shear stress above and below this mobilized zone:

$$\begin{aligned} T_{xmd,i} &= 2 \cdot \int_A \tau_S \, dA \cdot n_g = 2 \cdot \int_A \sigma_n \cdot \tan\varphi_S \, dA \cdot n_g \\ &= 2 \cdot \sigma_n \cdot \tan\varphi_S \cdot d_{O,l} \cdot \text{mob } L\left(u_{i-1}\right) \cdot n_g \end{aligned} \quad (3)$$

where A = mobilized area of passive earth resistance, φ_S = mobilized internal friction angle of the soil, $d_{O,l}$ = aperture width between two longitudinal tensile members, and mob $L(u_{i-1})$ = mobilized length of passive earth resistance.

The model was programmed using the software Matlab (version R2013b) and basically consists of two loops, an inner loop for the integration along the geogrid and an outer loop for modeling of different deformation states k. During the activation phase, in each step an additional element is switched on along the geogrid. Once the entire geogrid is activated, for each step, the displacement of the last element n at the free end is increased by an incremental displacement u_{inc}. Integration is then carried out from the free end, as both, displacement ($u_{k+1,n} = u_{k,n} + u_{inc}$) and force ($T_{k,n} = 0$), boundary conditions are known there, to the loaded end,. This has the particular advantage that the simulations can be carried out without using test results, e.g. force and displacement at clamp (of course using input functions evaluated from special tests as described in the next section).

2.2 *Input functions*

To solve Equations 1 to 3 some input functions are necessary, which are described in this section. The first input function describes the geogrid load-strain behavior, if necessary, including its creep characteristics by using isochronous curves and its strain-rate dependency. For modeling pullout tests with PET geogrids, it was found to be sufficient to use piecewise linear approximations of short-term tensile test results, as shown in Figure 1b (top). Additionally, the junction strength has to be defined as input for the model. For modeling laid geogrids with welded junctions, the junction strength was determined by tests according to GRI-GG2 (2005) with constrained rotation.

For the development of the other necessary input functions, pullout tests on modified geogrid specimens were carried out in the pullout test device shown in Figure 1a (top) with dimensions of 43.5 × 30 × 20 cm (L × B × H). The mobilization of the stress-dependent contact friction angle between longitudinal tensile members and soil has been evaluated using specimens without any transverse tensile members, so-called S0 tests. Besides the stress dependency, it has been found that the contact friction angle strongly depends on the soil density.

To determine the mobilization of the bearing resistance in front of transverse tensile members, results from pullout tests using specimens with one (S1) and without any transverse tensile members (S0) have been compared. Thereby, the development of a passive earth pressure zone with length mob L as in Figure 1c has been evaluated. To be used in Equation 3 with regular geogrid specimens (SV), this function of mobilized length has to be limited by the distance to the next transverse member, accounting for the interference between consecutive transverse members. This method from Ziegler & Timmers (2004) has the advantage that the bearing resistance is not regarded as an isolated mechanism (as e.g. by Teixeira et al. 2007), but includes its interaction with the mobilized friction on longitudinal tensile members. While the mobilized length is approximately independent of normal stress, it highly depends on the soil density.

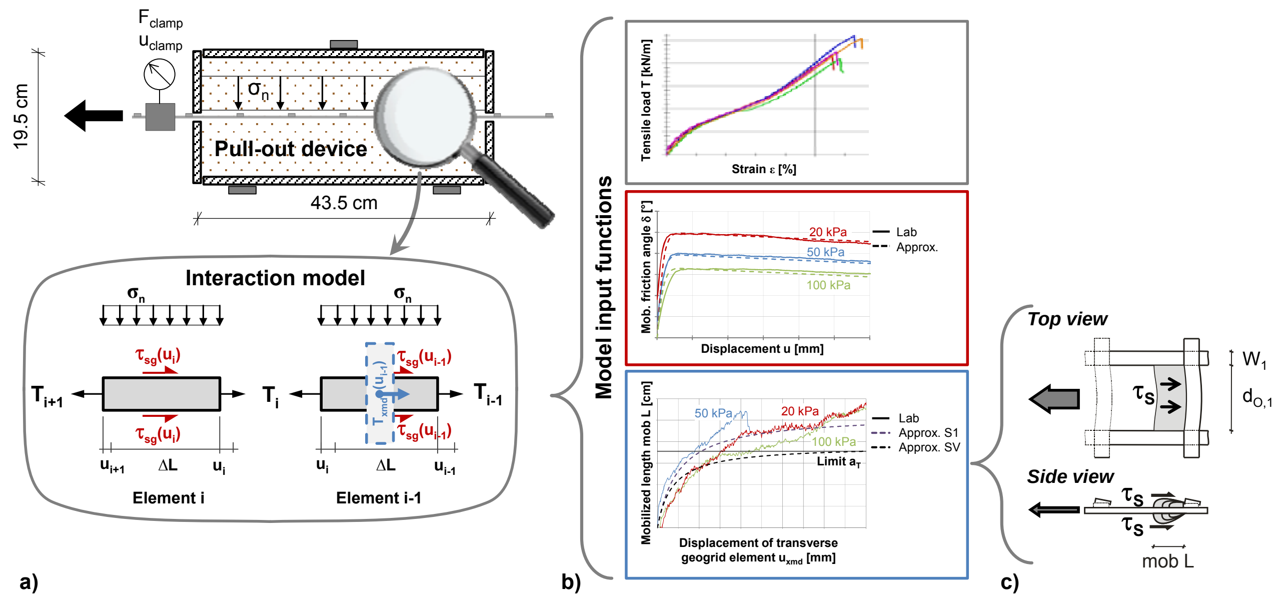

Figure 1: a) Interaction model with b) its input functions (after Jacobs et al. 2014) and c) its bearing model (after Ziegler & Timmers 2004).

2.3 *Model calibration with standard pullout tests*

As stated above, after having provided the input functions, each simulation of a pullout test runs independently of the results of the specific modeled test. Only the form of the function of mobilization length for regular specimens (see Equation 3) needs to be calibrated with the test results.

Figure 2a illustrates exemplarily model and test results of three test configurations with different normal pressures, but same soil (sand 0/2 with relative density $D_r = 31$ %) and same geogrid product (PET geogrid with tensile strength $T_f = 433$ kN/m and tensile stiffness $J_{0\text{-}2\%} = 8500$ kN/m). The curves represent the characteristic result of a pullout test, which is the measured force at the clamp T_{clamp} (i.e. the pullout resistance) versus the displacement at the clamp u_{clamp}.

Without being able to present all test and model results here, it can be stated that, after calibration of the mobilized length function for regular specimens, the interaction model matched all test results from the vast test program reasonably well. Only few tests in medium-dense and dense gravel (highly dilative) required the introduction of an additional calibration parameter to account for the constrained horizontal dilation within the standard pullout box.

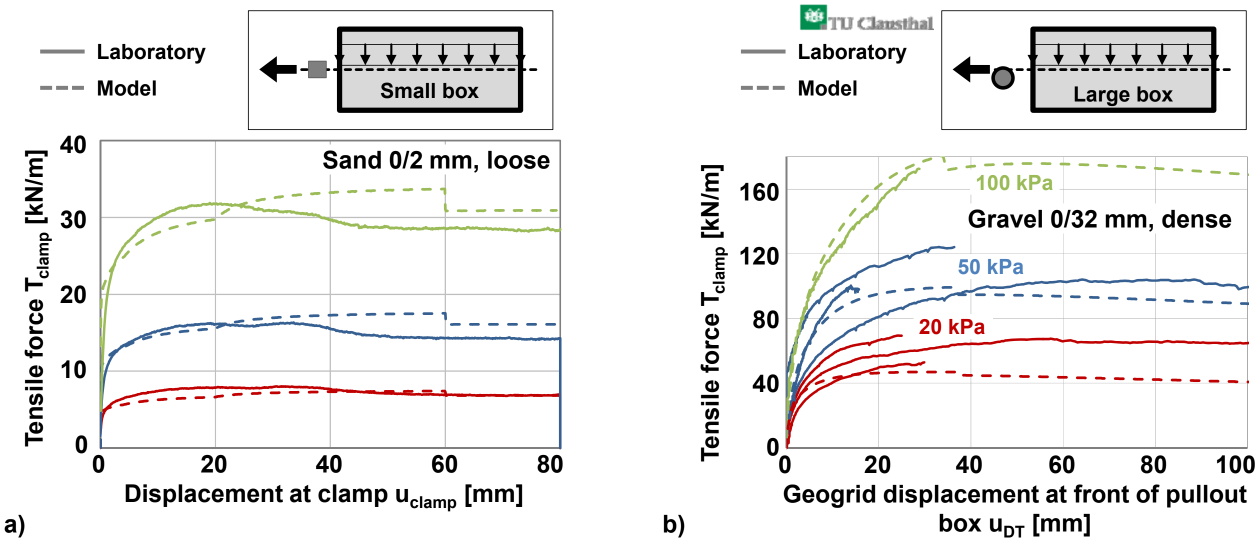

Figure 2: Results of a) model calibration with standard pullout tests and b) model validation with large pullout tests (after Jacobs et al. 2014).

2.4 *Model validation with large pullout tests*

The developed interaction model has been validated with results from tests, which were carried out with the same materials as for the model development but in a large pullout box at the Technical University of Clausthal, Germany (Meyer & Holm, 2012). This pullout box had dimensions of 150 × 60 × 60 cm (L × W × H) and allowed for a geogrid anchorage length of 120 cm. All tests were conducted with a gravel (particle diameters 0/32 and $D_r = 73$ %) and with a geogrid (regular PET geogrid with tensile strength $T_f = 233$ kN/m and tensile stiffness $J_{0\text{-}2\%} = 4300$ kN/m), which had also been used for development of the model input functions. Figure 2b shows the resulting development of the pullout resistance with increasing pullout displacement of various tests at three different normal pressures σ_n and the corresponding model results. In spite of some variance in results of repeated tests (20 and 50 kPa) due to the large test box, on average, the model has reproduced the test results well, for both, mobilization and maximum pullout resistance. Furthermore, the model could be validated by strain and displacement distributions, measured with strain gauges and displacement transducers connected to the geogrid using tell-tails, respectively, as presented in Jacobs et al. (2014).

Overall, the interaction model has successfully been validated with results from tests in a large pullout box, using input parameters derived from tests in a small test box. Therefore, the model has been ready to be transferred to the boundary value problem of geogrid pullout within anchorage trenches.

3 MODEL UPGRADE FOR ANCHORAGE TRENCHES

Wherever geogrids as reinforcement take up loads, these loads have to be transferred to the surrounding soil, i.e. the geogrids have to be anchored. Especially within reinforced veneer cover systems, e.g. as shown in Figure 3a for a surface sealing of a waste disposal site, high tensile geogrid loads occur that have to be anchored at the crest of the slope. To achieve anchorage of high loads while covering a small horizontal area, so-called anchorage trenches are used, as in the right of the photograph in Figure 3a and as sketched in Figure 3b. In such trenches, the geogrid alignment is not horizontal but deviated, which, in contrast to the boundary value problem of a pullout test, causes non-uniform stress distributions and deviation effects. Therefore, to be able to model the interaction of geogrid and soil within an anchorage trench, the developed interaction model had to be upgraded accordingly as follows.

3.1 *Incorporation of non-uniform normal stress distribution*

Figure 3b shows that the overburden along the geogrid within an anchorage trench varies, which results in a non-uniform vertical stress distribution $\sigma_V(x)$. The inclination of the geogrid varies as well so that, according to e.g. Koerner (2012) or EBGEO (Deutsche Gesellschaft für Geotechnik 2011) the normal pressure on the geogrid is calculated by:

$$\sigma_n(x) = \sigma_v(x) \cdot \cos\beta(x) \tag{4}$$

where $\beta(x)$ = geogrid inclination along the anchorage length.

3.2 *Incorporation of deviation forces*

At the points of change in inclination along a geogrid, deviation effects occur. Up to date, deviation forces are neglected in the design of geogrid anchorage. For anchorage of geomembranes, Koerner (2012) proposed an increased normal pressure on the bottom side of the geomembrane along the first horizontal stretch (see Figure 3b) to take into account the vertical fraction of the tensile force at the crest, but only regarding the first deviation. For anchorage of geomembranes and geotextiles, SETRA & LCPC (2000) and Villard & Chareyre (2004) used Euler's and Eytelwein's equation of rope friction to reduce the tensile force at each deviation, which however, according to the experimental results of Briançon et al. (2000) led to an overestimation of the deviation effect. Therefore, in this study, a new model has been developed, which calculates the deviation forces from equilibrium, similarly as for a steel tendon within a prestressed concrete beam and which then defines an influence length for each deviation.

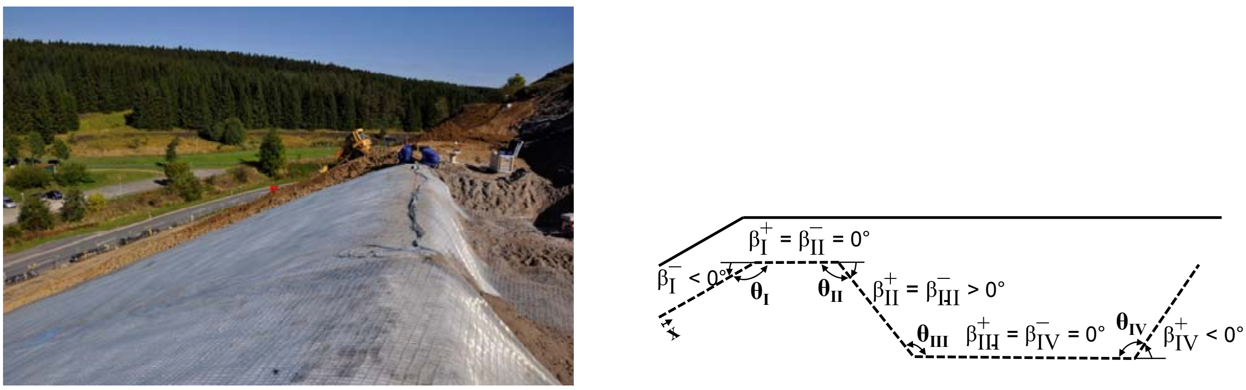

a) b)

Figure 3: a) Geogrid reinforced veneer cover system and b) sketch of a geogrid anchorage trench.

In Figure 3b a typical geogrid alignment within an anchorage trench is shown. The opening angle θ_j of each deviation j can be calculated by:

$$\theta'_j = 180° + \beta_j^- - \beta_j^+ \qquad (5)$$

$$\theta_j = \theta'_j \qquad \text{for } \theta'_j < 180° \qquad (6)$$

$$\theta_j = 360° - \theta'_j \qquad \text{for } \theta'_j > 180° \qquad (7)$$

where β_j^- and β_j^+ = geogrid inclination from deviation j towards the slope and towards the free end, respectively.

For $\theta'_j < 180°$, the opening angle is directed downwards leading to a downward-directed deviation force and therefore called deviation thrust, while for $\theta'_j > 180°$ an upward-directed deviation force is caused, being called deviation uplift.

Cutting the geogrid left and right of a deviation as drawn in Figure 4a for the downward-directed deviation or in Figure 5a for the upward-directed deviation, force equilibrium gives the deviation force vector:

$$\underline{F}_{D,j} = \underline{T}_j^- + \underline{T}_j^+ \qquad (8)$$

where $\underline{T}_j^-$ and $\underline{T}_j^+$ = tensile geogrid force vector from deviation j towards the slope and towards the free end, respectively.

Using the law of cosines with the tensile force values and its directions, the deviation force value is calculated by:

$$F_{D,j} = \sqrt{T_j^{-2} + T_j^{+2} - 2 \cdot T_j^- \cdot T_j^+ \cdot \cos\left(\beta_j^+ - \beta_j^-\right)} \qquad (9)$$

The deviation force surely does not act at a discrete point but spreads across a certain length. In accordance with the theory for steel tendons and with the membrane theory (e.g. Giroud & Noiray 1981) a circular arc is assumed, where a constant deviation stress acts. Division of the deviation force by the arc length, called deviation influence length $L_{D,j}$, gives the additional average stress caused by the deviation:

$$\sigma_{D,j} = \frac{F_{D,j}}{L_{D,j}} \qquad (10)$$

Regarding the determination of the influence length and the effect of the deviation stress for the interaction, the two cases of deviation thrust and deviation uplift have to be differentiated.

3.2.1 *Deviation thrust*

For the deviation thrust, the tensioned geogrid deforms towards the underlying soil, which is assumed to occur linearly with deviation stress $\sigma_{D,j}$ and the subgrade modulus k_s. This assumption together with some geometric calculations (which are not shown here due to limited space) leads to a non-closed solution for the deviation stress:

$$\sigma_{D,j} = \frac{F_{D,j} \cdot k_s \cdot \left(1 - \sin{}^{\theta_j}\!/_2\right)}{\sigma_{D,j} \cdot \cos\left(\gamma_j^+ - {}^{\theta_j}\!/_2\right) \cdot \sin{}^{\theta_j}\!/_2 \cdot \left(180° - \theta_j\right)} \qquad (11)$$

where γ_j^+ = angle between T_j^+ and $F_{D,j}$ as in Figure 4a.

After having solved Equation 11 iteratively, the influence length can be calculated using Equation 10. Finally, the normal fraction of the deviation stress is added to the normal pressure on the bottom side of the geogrid along the determined influence length as in Figure 4b and similar as by Koerner (2012) for geomembranes.

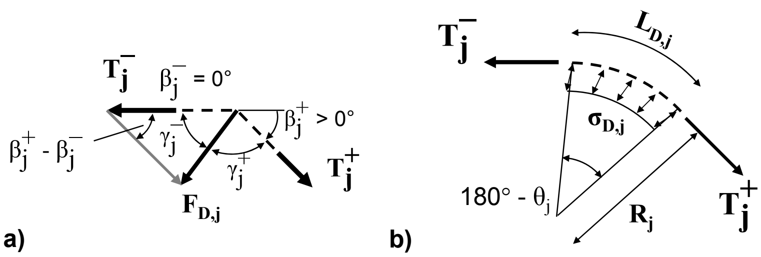

Figure 4: Downward-directed a) deviation force from equilibrium and b) deviation stress along circular influence length.

3.2.2 *Deviation uplift*

For the deviation uplift, the upward directed deviation force acts against the weight of the overlying soil block. The influence length $L_{D,j}$ from Equation 10 can therefore be derived from vertical equilibrium as in Figure 5b:

$$F_{D,v,j} = W_j\left(L_{D,j}\right) + T_{s,j}^-\left(L_{D,j}\right) + T_{s,j}^+\left(L_{D,j}\right) \qquad (12)$$

where $F_{D,v,j}$ = vertical portion of the deviation force $F_{D,j}$, $W_j(L_{D,j})$ = weight of overlying soil block, depending on influence length $L_{D,j}$, and $T_{s,j}^-$ and $T_{s,j}^+$ = shear forces on lifted soil block as in Figure 5b, also depending on influence length $L_{D,j}$.

Along the resulting influence length $L_{D,j}$, the overlying soil block is lifted and accordingly no contact is set on the bottom side of the geogrid to the underlying soil, again in accordance with membrane theory (e.g. Espinoza 1994).

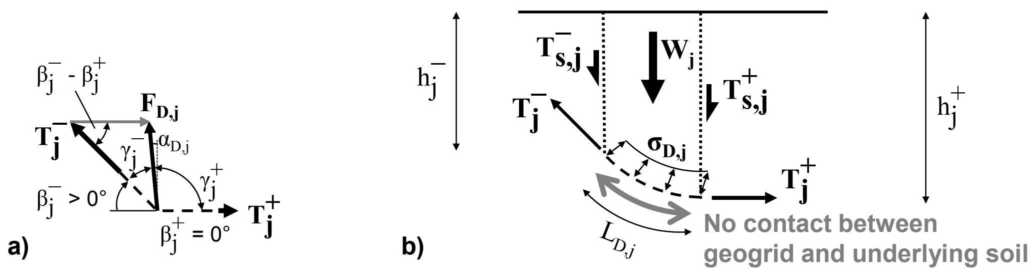

Figure 5: a) Upward-directed deviation force from equilibrium and b) vertical force equilibrium for determination of circular influence length.

4 VALIDATION OF MODEL WITH FIELD MEASUREMENTS IN ANCHORAGE TRENCH

During the redevelopment of the waste disposal site *Pochsandhalde Zellerfelder Tal*, Clausthal-Zellerfeld, Germany in 2010, a geogrid reinforced surface sealing system was constructed. In the course of construction, as shown in Figure 6, one geogrid roll was instrumented with strain gauges within the anchorage trench by the Technical University of Clausthal, Germany (Meyer and Holm 2010) to record the load transfer from geogrid to surrounding soil. The measurements have been used to validate the developed interaction model, including the deviation force approach, within an anchorage trench as described in this section.

The sketch in Figure 6 shows the geometry and the used soils of the instrumented anchorage trench. The *Pochsand* was installed with a comparable density and a similar geogrid was used as in the pullout test shown in Figure 2a. Therefore, after considering a reduced geogrid stiffness due to creep, the developed input functions could be used for modeling pullout within this anchorage trench. To take into account the effect of the first deviation at x' = 0 m, some part of the slope has been included into the anchorage trench model as shown by the sketch in Figure 6.

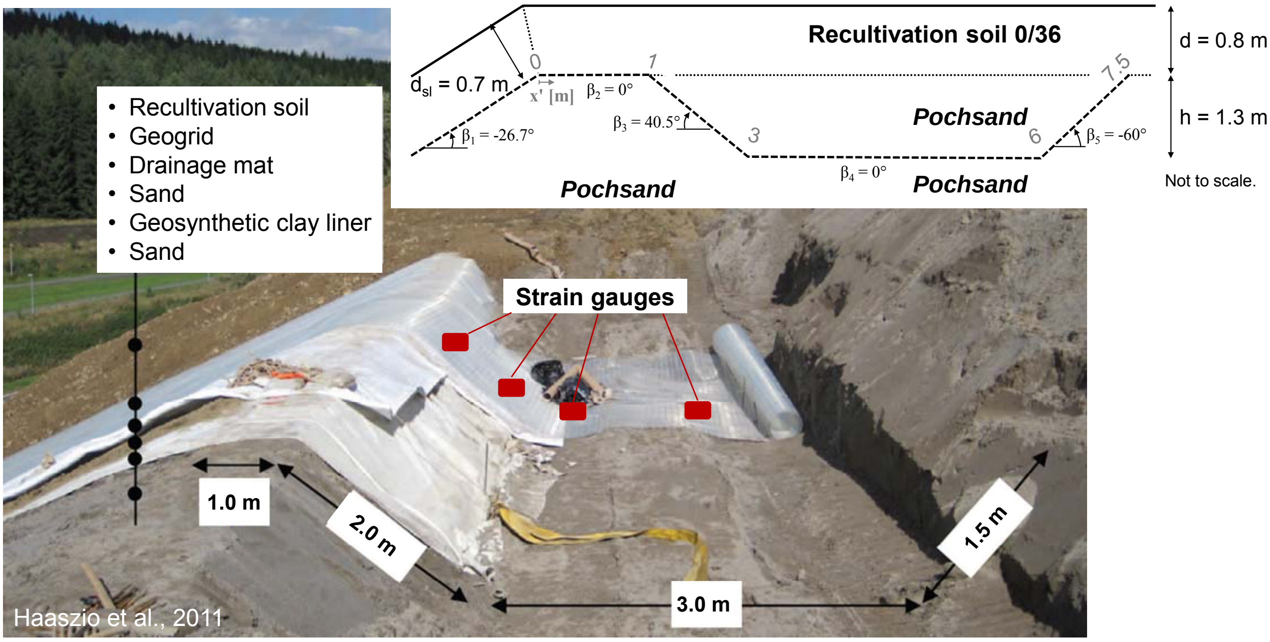

Figure 6: Instrumented geogrid anchorage trench at waste disposal Pochsandhalde Zellerfelder Tal, Germany.

In Figure 7, the measured geogrid strains are shown for three loading states along the anchorage length of the geogrid. The first two states were recorded during construction of the slope, while the last measurement at 1080 min after termination of the anchorage trench was recorded after termination of the entire slope construction at maximum loading (Vollmert et al. 2012). The strain curves resulting from the modeled anchorage trench are also illustrated in Figure 7. They are in good agreement with the measured strains, what was reached without changing any of the parameters derived from the laboratory tests but including the approach for the deviation effects. These effects can be seen clearly in the strain distributions. The first two deviations as deviation thrusts have caused an additional pressure on the bottom side of the geogrid, leading to more load transfer, which is equal to higher gradients in the strain distributions. At the third deviation, for the last loading state, a small soil block has been lifted so that there is no contact between the bottom side of the geogrid and the soil, leading to a smaller gradient in the strain distribution.

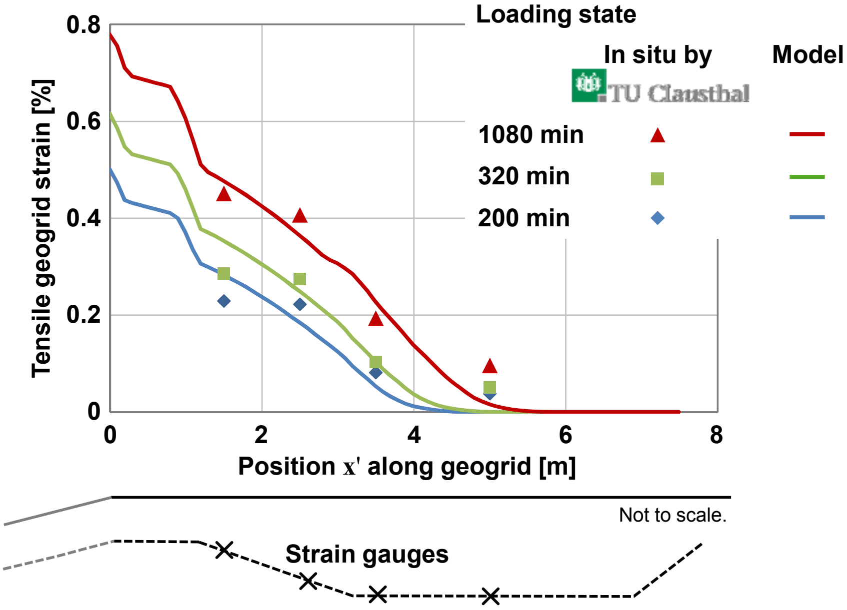

Figure 7: Measured and modeled geogrid strains of instrumented anchorage trench.

5 SUMMARY AND CONCLUSIONS

It was described that the current design of geogrid anchorage under the assumption of a constant interaction coefficient along the entire anchorage length and neglecting effects of deviations as in trenches is simplifying the real behavior. Against the background of a required proof of service life greater than 100 years e.g. for structures on waste disposal sites in Germany, it is necessary to explicitly take into account the complex interaction behavior and deviation effects, when regarding anchorage trenches with low overburden.

Therefore, a geogrid anchorage trench model was developed taking the followings steps:

- Development of an interaction model with its input functions and model calibration varying soil type (sand and gravel), soil density, geogrid tensile strength and stiffness, geogrid aperture size and overburden pressure.
- Model validation with large pullout tests without observation of any size effects.
- Formulation of an approach to account for deviation effects and incorporation into interaction model.
- Validation of entire model using in situ measurements from an instrumented anchorage trench.

With the presented interaction model, it is possible to solve the statically indetermined geogrid anchorage taking into account the displacement boundary conditions and the nonlinear interaction. The model calculates the displacement, strain and force distributions as well as the junction loads along the geogrid for any input geogrid action, enabling a direct comparison of the loading of all geogrid components with their material resistances. Therefore, with the model, not only the ultimate limit state, but also all statically and deformation compatible serviceability limit states can be regarded.

In a next step, an extensive parameter study is carried out comparing modeled anchorage trench resistances with resistances from current design codes. Depending on the resulting differences, limits will be formulated for a safe use of current codes or a new design approach will be developed for either safe or more efficient design of geogrid anchorage with trenches.

ACKNOWLEDGMENTS

The author would like to thank the team from Naue GmbH & Co. KG for their input and their financial support.

REFERENCES

Briançon, L., Girard, H., Poulain, D. and Mazeau, N. (2000) Design of anchoring at the top of slopes for geomembrane lining systems. *2nd European Geosynthetics Conference, EuroGeo 2000*, Bologna, Italy, Pàtron editore, Bologna, Italy, 2, 645-650.

British Standard, B.S. 8006-1 (2010) *Code of practice for strengthened/reinforced soils and other fills*.

Bundesanzeiger Verlag (2009) *Verordnung über Deponien und Langzeitlager (Deponieverordnung – DepV, Landfill Ordinance)*, 27.04.2009 BGBl. (Federal Law Gazette), lang.: German.

Deutsche Gesellschaft für Geotechnik (German Geotechnical Society) (2011). *EBGEO: Recommendations for Design and Analysis of Earth Structures using Geosynthetic Reinforcements*, Ernst & Sohn, Berlin.

Espinoza, R.D. and Bray, J.D. (1995) An Integrated Approach to Evaluating Single-Layer Reinforced Soils, *Geosynthetic International*, **2**, 4, 723-739.

Ezzein, F.M. and Bathurst, R.J. (2014) A new approach to evaluate soil-geosynthetic interaction using a novel pullout test apparatus and transparent granular soil, *Geotextiles and Geomembranes*, **42**, 3, 246-255.

Giroud, J.P. and Noiray, L. (1981) Geotextile-reinforced unpaved road design. *Journal of the Geotechnical Engineering Division*, ASCE, **107**, 9, 1233-1254.

GRI-GG2 (2005) Individual Geogrid Junction Strength, Rev. 3. Geosynthetic Research Institute, Philadelphia, USA.

Haaszio, S., Werth, K. and Tebbe, J. (2011) Sanierung Pochsandhalde Zellerfelder Tal, Planung und Ausführung eines 1:2 geneigten Oberflächenabdichtungssystems unter Einsatz von hochzugfesten Geogittern. *7. Leipziger Deponiefachtag. „Stilllegung, Sicherung, Nachsorge und Nachnutzung von Deponien“*, Leipzig, Germany, lang.: German.

Jacobs, F., Ziegler, M., Vollmert, L. and Ehrenberg, H. (2014) Explicit Design of Geogrids with a Nonlinear Interface Model, *10th Intern. Conf. on Geosynth.*, *10ICG*, Berlin, Germany.

Koerner, R.M. (2012). *Designing with Geosynthetics*, **2**, 6. Ed., Xlibris Corporation, USA.

Meyer, N. and Holm, B. (2010) Prüfbericht - Untersuchung der auftretenden Geogitterdehnungen im Verankerungsgraben der „Pochsandhalde im Zellerfelder Tal“, *Institute of Geotechnical Engineering and Mine Surveying*, Technical University of Clausthal, Germany, lang.: German (unpublished).

Meyer, N. and Holm, B. (2012) Prüfbericht - Untersuchung des Kraftverlaufes über die Einbindelänge bei Pull-Out Versuchen, *Institute of Geotechnical Engineering and Mine Surveying*, Technical University of Clausthal, Germany, lang.: German (unpublished).

Müller, W. (2014) Long-term pull-out resistance and material properties of geogrids. *10th Intern. Conf. on Geosynth.*, *10ICG*, Berlin, Germany.

Palmeira, E.M. (2009) Soil-geosynthetic interaction: Modelling and analysis. *Geotextiles and Geomembranes*, **27**, 368-390.

SETRA & LCPC (2002) *Guide Technique – Etanchéité par géomembranes des ouvrages pour les eaux de ruissellement routier- guide complémentaire*. Service d'Études techniques des Routes et autoroutes (SETRA) and Laboratoire central des Ponts et chaussées (LCPC), Paris, France.

Teixeira, S.H.C., Bueno, B.S. and Zornberg, J.G. (2007) Pullout Resistance of Individual Longitudinal and Transverse Geogrid Ribs, Journal of Geotechnical and Geoenvironmental Engineering, ASCE, **133**,1, 37-50.

US Department of Transportation (2001) Federal Highway Administration, Publication No. FHWA-NHI-00-043, *Mechanically Stabilized Earth Walls and Reinforced Soil Slopes*, Design and Construction Guidelines.

Villard, P. and Chareyre, B. (2004) Design methods for geosynthetic anchor trenches on the basis of true scale experiments and discrete element modelling. *Canadian Geotechnical Journal*, **41**, 1193-1205.

Vollmert, L., Werth, K., Emersleben, A. and Holm, B. (2012) In-Situ-Beanspruchungen eines Geogitters im Verankerungsbereich einer Oberflächenabdichtung am Beispiel der Pochsandhalde Zellerfelder Tal, *28. Fachtagung „Die sichere Deponie - Sicherung von Deponien und Altlasten mit Kunststoffen“*, Würzburg, Germany, lang.: German.

Ziegler, M. and Timmers, V. (2004) A new approach to design geogrid reinforcement. *3rd Europ. Geosynthetics Conf.*, *EuroGeo3*, Munich, Germany, 661-667.